NOTES AND CORRESPONDENCE

On the Use of Slow Ascent Meter-Scale Sampling (SAMS) Radiosondes for Observing Overturning Events in the Free Atmosphere

BEN B. BALSLEY

Cooperative Institute for Research in Environmental Sciences, University of Colorado, Boulder, Colorado

LAKSHMI KANTHA

Department of Aerospace Engineering Sciences, University of Colorado, Boulder, Colorado

WILLIAM COLGAN

Cooperative Institute for Research in Environmental Sciences, University of Colorado, Boulder, Colorado

(Manuscript received 1 April 2009, in final form 7 December 2009)

ABSTRACT

This note describes the development of a method for obtaining high vertical resolution (meter scale) measurements of basic meteorological quantities and turbulent overturns, using radiosondes with slow ascent rates. Although the method has some limitations, it can provide profiles of standard atmospheric variables from the surface to more than 20 km, with significantly improved vertical resolution. It can also help better identify regions of turbulent overturns. This correspondence presents some initial results demonstrating the occurrence of relatively small-vertical-scale overturns throughout the entire atmospheric column.

1. Introduction

It is becoming increasingly clear that an improved understanding of the causal mechanisms underlying the generation of finescale turbulence in the atmosphere requires sampling the atmosphere at vertical scales of a few meters or less (Werne and Fritts 1999; Fedorovich et al. 2004; Fritts et al. 2009a,b; Balsley et al. 2008; Tjernström et al. 2009). Typically, operational radiosonde data have been archived at the ''mandatory levels'' (i.e., the surface and pressure levels of 1000, 925, 850, 700, 500, 400, 300, 250, 200, 150, 100, 70, 50, and 10 mb), plus additional ''significant levels'' (viz., pressure levels where there are significant changes in either the temperature or the dewpoint temperature). More recently, these data are being archived at 6-s sampling rates, while, in a few instances, data are being recorded using 2-s resolution. Although this is sufficient to reproduce the gross features of a sounding for most applications, it is clearly insufficient for examining the small-scale details that contain important information on the source of locally generated turbulence (e.g., small-scale gravity waves, frontal passages, and local wind gusts).

The need for improved vertical resolution in atmospheric measurements has been met from time to time by mounting specialized campaigns. During these periods, radiosonde data are archived at much higher (1–2 s) sampling rates. Examples of such campaigns include the Fronts and Atlantic Storm Tracks Experiment (FASTEX) and the Terrain-Induced Rotor Experiment (T-REX). The FASTEX data were gathered using conventional radiosondes sampled at 6-s intervals, with some additional measurements made at 2-s intervals. For a typical radiosonde ascent rate of around 5 m s^{-1}, the resulting vertical resolution during FASTEX ranged between 10 and 30 m. The radiosonde sampling rate during T-REX, on the other hand, was fixed at one sample per second, corresponding to a vertical resolution of ~5 m (Wang et al. 2009).

Corresponding author address: Ben B. Balsley, Cooperative Institute for Research in Environmental Sciences, University of Colorado, Boulder, CO 80309.
E-mail: balsley@cires.colorado.edu

DOI: 10.1175/2009JTECHA1310.1

Although the vertical resolutions during these campaigns are a clear improvement for examining small-scale atmospheric features, recent observations and models have pointed to the need for even higher-resolution sampling. For example, recent in situ measurements reported by Balsley et al. (2008) and Tjernström et al. (2009) using the University of Colorado (CU) tethered lifting system (TLS) showed the dimensionless gradient Richardson number Ri in the first 1000 m of the atmosphere to be strongly scale dependent. These authors showed that, typically, although the lowest 1–2 km of the atmosphere is dynamically stable ($0.4 < \mathrm{Ri} < 0.7$) when measured on vertical scales of 100 m or more, it becomes more and more unstable when viewed at increasingly smaller scales. In fact, Ri values at vertical scales of ~2 m show that a major fraction (>60%) of the entire region examined exhibits Ri values < 0.25. Similar but less detailed results for the troposphere have been reported by Cho et al. (2003). Clearly, this type of finescale analysis is not possible using datasets that have only 10–30-m resolution.

In a separate analysis, Clayson and Kantha (2008) have reported results illustrating the potential for deducing turbulence levels, mixing, gradient Richardson numbers, and atmospheric overturning in the free atmosphere using the 2-s FASTEX data collected during 1997 and 6-s data taken at Tallahassee, Florida, and Denver, Colorado, during 2005. Based on their analyses, these authors stressed the need for higher vertical-resolution sampling using slow-ascent-rate radiosondes recording at 1-s intervals or better to sample the smaller turbulence scales and better deduce the dissipation rates of turbulence kinetic energy in the free atmosphere.

Recent modeling results (D. Fritts 2009, personal communication) show the response of local small-scale vertical shears to the presence of a propagating atmospheric gravity wave. In the compressive phase of the wave, the small-scale shears are enhanced, and these enhanced shears, in turn, generate regions of enhanced turbulence. This process appears to operate on vertical scales of a few tens of meters or less, where the existing shears are most pronounced, and they provide additional evidence for the need for high-resolution measurements.

In view of the growing need for higher vertical-resolution measurements as outlined earlier, it is appropriate to examine the current radiosonde technology to determine if it can be extended to provide higher-resolution measurements, even if such measurements turn out to be possible under somewhat restricted conditions. The obvious methods for increasing vertical resolution are either 1) by increasing the sampling rate and/or 2) by decreasing the balloon ascent rate. In addition, for a technique to be successful, the resulting system must be relatively simple and robust.

Pertinent aspects of a recent preliminary study toward this end by the Cooperative Institute for Research in Environmental Sciences (CIRES) at CU are outlined later. Briefly, these initial results demonstrate that, with certain restrictions, it is possible to achieve ~1-m vertical-resolution measurements from the surface to altitudes in excess of 20 km using slow-rise-rate radiosondes. This emerging technique has been termed the slow-ascent meter-scale sampling (SAMS) radiosonde technique. Although this technique has some limitations and the potential accuracy of the measurements cannot be assessed using this limited dataset, it appears that it provides significantly better vertical resolution than that currently available. Potential problems, design considerations, and initial results are outlined below.

2. Modifying conventional radiosondes to achieve high-resolution measurements: Potential problems

A brief description of a number of potential problems that could arise in the process of modifying conventional radiosonde systems for high-resolution sampling is presented below.

a. The use of faster sampling rates

It is reasonable to expect that conventional radiosonde systems operating at less than 1 sample per second are limited by design considerations to these values. It is also reasonable to expect that the information regarding these limitations is proprietary and could involve either data rate limitations (bandwidth) or limitations associated with the sensor response times. For example, although the Väisälä RD93 dropsonde quotes a faster sampling rate of 2 samples per second, the inherent time response of the temperature sensor is quoted at 2.5 s, implying a vertical resolution at a nominal 12 m s^{-1} descent rate of ~31 m at sea level, with correspondingly poorer resolution at higher altitudes (Hock and Franklin 1999). The RS90 sonde, on the other hand, has published response times of 0.2 and 0.5 s at 1000 and 10 hPa, respectively, whereas the RS92 sonde used in the current tests has response times of 0.4 and 2.5 s at 1000 and 10 hPa, respectively. Both RS90 and RS92 results are quoted for a 6 m s^{-1} flow. The reduced rise rates and correspondingly reduced flows in the SAMS launches will result in slower response times. It follows that faster sampling would likely require redesigning the sensor package. Although this is a real possibility, the point of the present study is to use available systems and not to attempt an extensive redesign. We have, therefore, ignored this possibility and have concentrated instead on developing slower radiosonde ascent rates.

b. The use of slower ascent rates

Vertical velocities in the daytime atmosphere can, even under relatively weak convective conditions, extend to values that are a significant portion of or greater than the ascent rate of a conventional radiosonde balloon. As a consequence, it is obvious that the use of slower-rise-rate radiosondes will have to be restricted to periods when significant updrafts and downdrafts are absent. This restriction limits the use of slower ascent-rate balloon systems to either quiet daytime conditions (minimal convection) or to nighttime operations and then only under relatively quiescent conditions. If these sondes could be launched above the planetary boundary layer (PBL), then the restrictions might be less severe, so that routine high-resolution sampling of the free atmosphere could become feasible.

One additional consideration that arises from the analysis of slow-rise-rate systems concerns the possible evolution of the air mass under study. Moreover, slower rise rates also result in greater horizontal distances covered to achieve the same altitude as a conventional system. These factors put a greater emphasis on the temporal evolution of the air mass under study as well as the effects of changing orography along the flight path. Although we note that these considerations are increasingly valid for the slower rise-rate systems, they are also valid for conventional systems. Virtually no balloon launch can be considered as an instantaneous vertical profile of the atmosphere. To illustrate this point, consider a conventional radiosonde launch ascending to 25 km at a rise rate of 5 m s^{-1} and a mean wind of 8 m s^{-1}. As it passes through 25 km, some 5000 s after launch, the sonde will have moved horizontally 40 km. The resulting conventional profile will be inclined from the vertical by 58°.

c. Range-related telemetry problems

A further consideration of a slow-rise-rate radiosonde technique lies with the increased downwind distance a slow-rise-rate system will travel before reaching its maximum altitude. For example, if one assumes an ascent rate of 1 m s^{-1}, a radiosonde would take ~7 h to reach an altitude of 25 km. Assuming a mean horizontal wind speed of 8 m s^{-1} at all heights, the radiosonde will have traveled a horizontal distance of about 200 km. This distance is some 5 times greater than that which would have resulted from a conventional radiosonde ascent. In the slow-rise-rate ascent situation, the resulting telemetry signal strength would be weaker by the square of this ratio (i.e., ~25 times weaker). Thus, decreased signal strengths arising from the increased ranges could be problematic.

d. Battery lifetimes

Another potential problem lies with battery lifetime. To attain profiles up to altitudes comparable to those attained by conventional radiosondes, a radiosonde ascending at 1 m s^{-1} must record and transmit data 5 times longer than a conventional system. Such extended operations, particularly given the extremely low temperatures aloft, could easily exceed battery design limitations, resulting in the loss of battery power. Under standard conditions, a conventional Väisälä sonde battery will last for about 2 h. Using the same radiosonde package, SAMS launches will need battery lifetimes 4–5 times longer. However, the additional weight of an extended battery package should not be a problem, because the reduced lift of a SAMS system can offset the increase by increasing the volume of the balloon.

e. Sensor limitations at reduced rise rates

Because radiosonde sensors have been optimized to operate at ascent rates of approximately 5 m s^{-1}, it is reasonable to anticipate that slower ascent rates might result in reduced measurement accuracies in some of the sensors. Problems could arise, for example, from the reduced airflow past the sensors (ventilation). This problem, if it is found to exist, could preclude the use of slower ascent-rate systems unless efforts are made to reduce such effects (e.g., by redesigning the sensor package).

f. Problems associated with balloon aerodynamics

There are at least two additional potential problems involved with employing slower rise-rate balloons to make high-resolution atmospheric measurements. Although both problems exist for all high-resolution balloon-borne measurements, they need to be reevaluated in the case of the slow-rise-rate systems.

One problem lies with the accuracy of the response of the instrument package to the relatively rapid components of wind fluctuations. Insofar as the radiosonde plus balloon package can be considered a two-body system with inertia, this is a relatively complex problem. The problem is further exacerbated by using a smaller (cross section) balloon. Clearly, the response of the entire balloon-sensor package will compromise the accuracy of short-term, small-scale velocity measurements. Analysis of these problems clearly lies beyond the scope of this preliminary study.

The second problem concerns the random, self-induced lateral motions exhibited by a balloon as it ascends through the air mass. These self-induced motions constitute an undesirable effect that needs to be minimized as much as possible. This problem has been addressed in MacCready (1965), who showed that these

motions are strongly dependent on the Reynolds number Re, where

$$\mathrm{Re} = \frac{nLr}{h},$$

where, ρ and η are the density and viscosity of the fluid, respectively; v is the balloon's velocity relative to the air, and L is the size of the object. In a comparison between different balloon characteristics, MacCready (1965) demonstrated that the smooth, expandable, neoprene balloons employed in typical radiosonde launches have subcritical Re values (i.e., greatly reduced self-induced motions) over the entire height range, provided that the nominal balloon diameter is $\leq\sim$90 cm. Larger diameter balloons result in supercritical Re values with associated large self-induced lateral motions beginning in the lower height ranges. At higher heights, Re values for a given balloon diameter transition from supercritical to subcritical values, with the height of this transition increasing with increasing balloon diameter. It follows that the reduced rise rates and smaller-diameter balloons used by the SAMS systems will have significantly smaller Re values and thus smaller self-induced motions, thereby providing improved accuracies over the entire height range.

3. System description and procedures

This investigation used Väisälä RS92-SGP radiosondes with dry 9.5-V (nominal) battery packs comprised of six AA-type batteries connected in series. These units operate between 400 and 406 MHz and transmit observations every second to a Väisälä MW21 ground receiver unit, where the data are processed using Väisälä proprietary software (DigiCORA version). These units come with factory-calibrated pressure, temperature, and relative humidity sensors with published total-sounding accuracies of ±1 hPa, ±0.5°C, and ±5%, respectively. The sensors have reproducibility in sounding accuracies of ±0.5 hPa, ±0.5°C, and ±2%, respectively (Väisälä Corporation 2006). Prior to launch, each radiosonde unit was reconditioned using a standard GC25 Väisälä ground check console. The reconditioning chamber heats the twin humidity sensors and the temperature sensor in a chamber with minimal humidity to remove possible contamination that may have accumulated on the sensor heads during storage and transport.

The RS92-SGP units also contain a 12-channel global positioning system (GPS) antenna. This allows the radiosonde unit to transmit its location back to the ground receiver unit every second. Proprietary code-correlating Väisälä software uses input from a secondary GPS base station at the launch site to differentially correct the location of the radiosonde to a horizontal positional uncertainty of 10 m. Radiosonde altitude can be determined using either the pressure sensor or the GPS position data. The DigiCORA software uses changes in GPS location to compute the north–south and east–west horizontal wind components with a stated uncertainty of 0.2 m s^{-1}. The horizontal navigational accuracy is stated as 10 m, while the corresponding vertical accuracy is quoted as 20 m.

It is important to point out at this point that the results shown below are primarily concerned with relative rise rates and not with the absolute altitude accuracy. In view of the nearly constant rise rates exhibited in the SAMS profiles, combined with the differential accuracy of the Väisälä system, it is our opinion that the relative accuracy of the 1-s altitude values provides a more than reasonable estimate for the current purposes. Of course, quantification of this accuracy must await a more extensive study.

The launch site used in this investigation was the Boulder Atmospheric Observatory (BAO), a National Oceanographic and Atmospheric Administration (NOAA) facility located at Erie, Colorado (40.05°N, 105.00°W), at an elevation of 1576 m above mean sea level. A total of 19 experimental SAMS radiosondes were released from this location during July and August 2008. Ultra-high-purity helium gas was used to inflate the radiosonde balloons to provide lift.

The Väisälä ground receiver unit was initially connected to a conventional linear dipole-antenna array (denoted herein as dipole) to receive the data transmissions from the radiosonde unit. After experiencing some signal dropouts during the initial launches, a multielement Yagi-Uda antenna was employed for subsequent launches. The use of the Yagi-Uda antenna greatly improved system directivity and gain.

Net lift of the entire balloon/radiosonde package was determined by tethering both the helium-filled balloon and the ~285-g RS92 package to the platform of an Ohaus model TP4KD electronic scale capable of measuring both positive and negative forces. Net lift was measured inside the Erie facility building to eliminate the influences of wind gusts. Although the scale readings had a published accuracy of ±0.01 g, a more reasonable estimate of the actual accuracy was about ±5 g, in view of the presence of errant drafts in the building. Once a radiosonde package was calibrated to the approximately correct net lift plus a few grams, final changes were accomplished by attaching small (20 mg) ballast weights. Following this procedure, the package was taken outdoors, allowed to equilibrate to the ambient temperature, and then released.

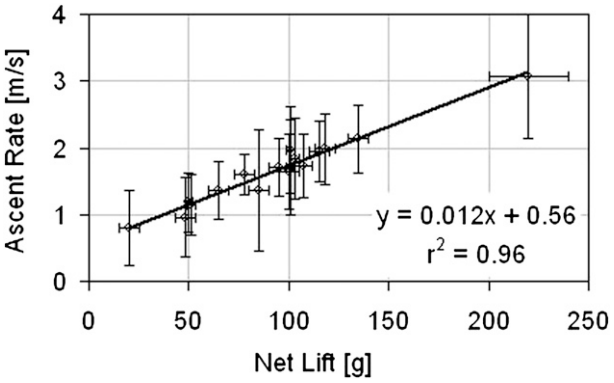

FIG. 1. Plot of the mean ascent rate of SAMS radiosonde as a function of net lift. Vertical error bars represent the standard deviation in ascent rate over the entire profiles, whereas the horizontal error bars represent uncertainty in net lift.

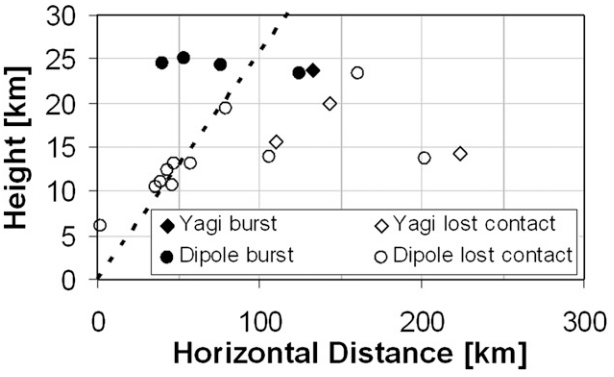

FIG. 2. Plot of the maximum heights and horizontal distances attained by each of the SAMS launches. These results are based on telemetered signals obtained during each flight. The dashed line represents an elevation angle of 15° from the launch site. See the text for details.

4. Initial results

a. Rise rate versus lift

The result of a series of 19 SAMS launches designed to investigate the relation between mean ascent rate and net lift appears in Fig. 1. Net balloon lift was determined by measuring the upward force on the entire package (balloon, radiosonde, and ballast), as described above. Mean ascent rates for these tests were carefully estimated using two separate techniques. The first technique involved fitting a least mean square fit straight line to the height versus time curves over each entire ascent.[1] The second technique involved calculating ascent rate from the archived 1-s GPS-derived radiosonde positions over the entire flight. Both techniques produced ascent rates that agreed to within $\sim$0.1 m s^{-1}.

The rise-rate data shown in Fig. 1 were obtained using the second procedure. The vertical error bars represent the standard deviation in ascent rate for each flight. Examination of Fig. 1 shows a reasonably linear relationship between mean ascent rate and net lift. Note that the net lift value for a conventional $\sim$5 m s^{-1} radiosonde ascent rate would be off scale in this figure. An analytical expression for the linear least mean square fit to the data points, as well as its r^2 value, has been included. The resulting line slope suggests an increase of 1.2×10^{-2} m s^{-1} in mean ascent rate for each 1-g increase of net lift.

[1] Somewhat surprisingly, reduced-lift balloon rise rates tended to be reasonably constant with height. Some indication of this feature can be noted also in Fig. 1 of MacCready (1965), who points out that, for smooth neoprene balloons with a constant drag coefficient, rise rate is proportional to $(r_o/r)^{1/6}$ (i.e., relatively constant over the height range).

b. Signal loss problems

Many of the 19 SAMS flights used in the SAMS tests unexpectedly lost signal strength before achieving their expected altitude of >20 km. This feature is illustrated in Fig. 2, where telemetered signal characteristics from all 19 launches have been plotted as a function of horizontal distance from the launch site versus altitude. Data points have been classified into four categories: 1) the filled circles denote dipole-tracked radiosondes that were observed to burst at altitude (bursting height was defined by the height at which data continued to be received but where the altitude values exhibited a rapid decrease); 2) the open circles denote dipole-tracked radiosondes that lost signal before bursting; 3) the single filled diamond denotes a Yagi-Uda-tracked radiosonde ascent where the balloon was observed to burst; and 4) the open diamonds denote Yagi-Uda-tracked radiosondes that lost signal before bursting. The dashed line represents the elevation angle (15°) of the first null of the theoretical antenna pattern when using the vertically polarized dipole antenna (radiosonde signals received at this elevation angle would be virtually undetectable).

Examination of Fig. 2 shows a number of informative features of the SAMS launches. The first feature to note is that all of the slow-rise-rate balloons that were observed to burst (all filled symbols) achieved maximum altitudes well in excess of 20 km. Second, eight of the lost radiosondes signals tracked using the dipole antenna (open circles) appear to ''clump'' around the 15° elevation angle shown by the dashed line. This clumping suggests that these particular radiosondes lost signal as they passed through the null of the dipole antenna pattern. Although these particular radiosondes may have continued to higher altitudes, they would have been assumed to have been lost, and no attempts would have

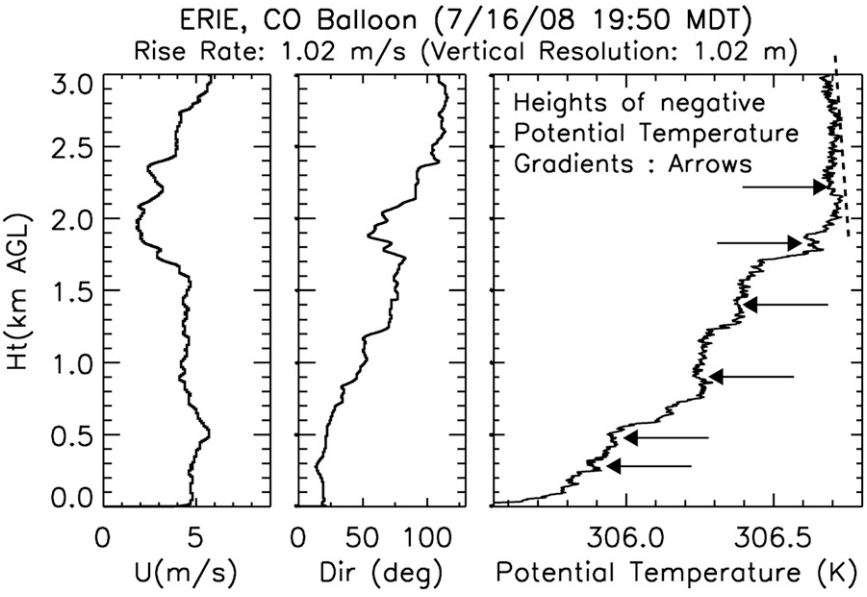

FIG. 3. Profiles of a SAMS nighttime ascent shown to only 3 km to better illustrate details of the high-resolution results. The mean ascent rate of this launch was 1.01 m s^{-1}. Arrows denote examples of vertically narrow regions that exhibit negative slopes in the potential temperature profile. The dashed line above 2 km suggests that the region between 2 and 3 km has a slightly negative slope.

been made to reacquire their transmissions. The third feature involves the remaining six radiosondes that neither burst nor approached the 15° null (all the remaining open symbols). It is reasonable to assume that the loss of signal in these instances may have arisen from the loss of battery power, because many of the launched sondes used batteries that inadvertently had been temporarily attached to other sondes during ground-based testing.

Finally, it might be surmised that radiosondes that traveled the largest horizontal distances could have lost contact by passing beyond the ''radar horizon.'' This assumption cannot be supported, because the ''worst case'' example is the data point on the right-hand limit of Fig. 2 at a range of ~220 km at an altitude of 13 km. At this height, the radar horizon would have been over 455 km (i.e., more than twice as far).

c. Initial profiles

Data for all the analyses described below have been extracted from an archived file containing unmodified standard 1-s Väisälä output values. One significant problem that was immediately apparent in this dataset was the absence of reliable humidity values, which exhibited unreasonable variations. Conversations with pertinent Väisälä representatives indicated that this was the result of insufficient ventilation at the reduced rise rates. There was no immediate ''fix'' to this problem. As a result, insofar as the analyses described below involve potential temperature calculations, they refer to actual potential temperature Θ and not to virtual potential temperature Θ_v.

An example of the high-resolution details available using the SAMS launches is shown in Fig. 3. This figure shows profiles of wind speed, wind direction, and potential temperature only between 0 and 3 km to provide some idea of the inherent vertical-resolution capability of these measurements.

The wind profiles in Fig. 3 show a relatively constant wind with height of about 5 m s^{-1} that changes direction from north-northeasterly at the surface to east-southeasterly at 3 km. Examination of the average potential temperature profile and ignoring for the moment the high-resolution fluctuations, the average value of the profile increases steadily through the nighttime stable boundary layer (SBL; i.e., from the surface to around 2 km), with a slope of about +0.6 K km^{-1}. Above the SBL top (defined as the height where the potential temperature slope decreases sharply), the slope can be seen to be roughly constant, with a slight, apparently negative slope (dashed line).

The horizontal arrows in the final panel identify a few examples of vertically narrow regions where the slope of the potential temperature profile exhibits small but significant negative excursions. Many additional negative slopes can be seen throughout this profile, some of

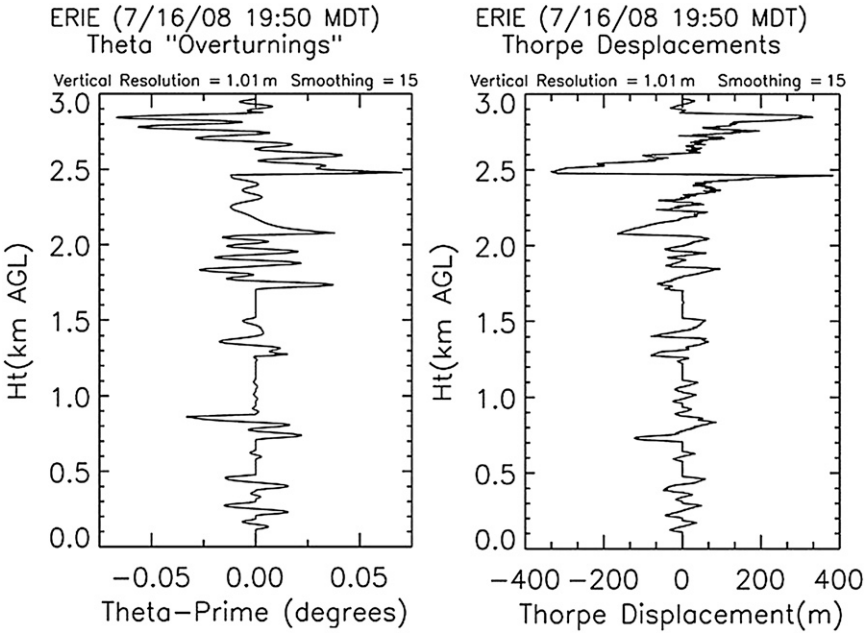

FIG. 4. Showing nonsmoothed potential temperature fluctuations and corresponding 10-point smoothed Thorpe scale displacements that arise from a reordering of the Fig. 3 potential temperature profile to produce a profile that is monotonically increasing with height.

which are quite small. The significance of these regions is discussed in the next section.

d. Examples of atmospheric overturning

One of the primary reasons for initiating this study was to examine high-resolution potential temperature profiles to look for overturning events and the resulting "Thorpe displacement" values (Clayson and Kantha 2008; Sorbjan and Balsley 2009). The concept of overturning was initially developed for oceanographic studies (Thorpe 1977; Alford and Pinkel 2000). The basic premise is that, under quiescent stable conditions, potential temperature profiles should increase monotonically with increasing height. This requirement arises because potential temperature profiles with negative slopes are statically unstable and cannot exist in the absence of external forcing. Profiles that exhibit negative slopes must therefore have been acted upon by external forces (e.g., atmospheric gravity waves or convective "bubbles") to produce these negative slopes. It is relatively easy to reorder these profiles to be monotonically increasing with height. It follows that the reordered profile provides a reasonable estimate of the profile that would have existed in the absence of perturbing forces. Furthermore, if account is taken of the vertical distances over which these reorderings take place, such distances can be considered to be a reasonable measure of the overturning height increment that produced each of the negatively sloped intervals.

Further evidence for the overturning events in Fig. 3 is illustrated in Fig. 4, which shows a profile of potential temperature fluctuations (θ') obtained by subtracting the measured potential temperature profile from the reordered profile. A corresponding profile of the Thorpe displacements appears in the right-hand panel. Examination of this figure shows the clear presence of temperature fluctuations of a few hundredths of a degree (K) and vertical scales of ± 50 to 100 m in the SBL, with larger (± 200 to 400 m) scales at higher heights. Many of these perturbations can be seen to correspond to the arrows shown at the lower heights in Fig. 3. Note that the extended, slightly negative slope in the upper heights (the dashed line in Fig. 3) is manifested in the Thorpe profiles as a region of continuously overturned region.

A second example of overturning is presented in Fig. 5 for a different SAMS launch, this time showing only the Thorpe displacement profile but over the entire height range of the ascent. Because this profile was obtained at a 2.1 m s^{-1} rise rate and has been smoothed by a 3-s (~6.3 m) running average for viewing convenience, some of the high-resolution details have been smoothed out.

Examination of Fig. 5 shows that, even in this smoothed presentation, typical Thorpe scales range between about ± 50 to ± 250 m throughout the entire height range. Interestingly, overturnings appear to be equally present in the troposphere and the stratosphere (i.e., above the

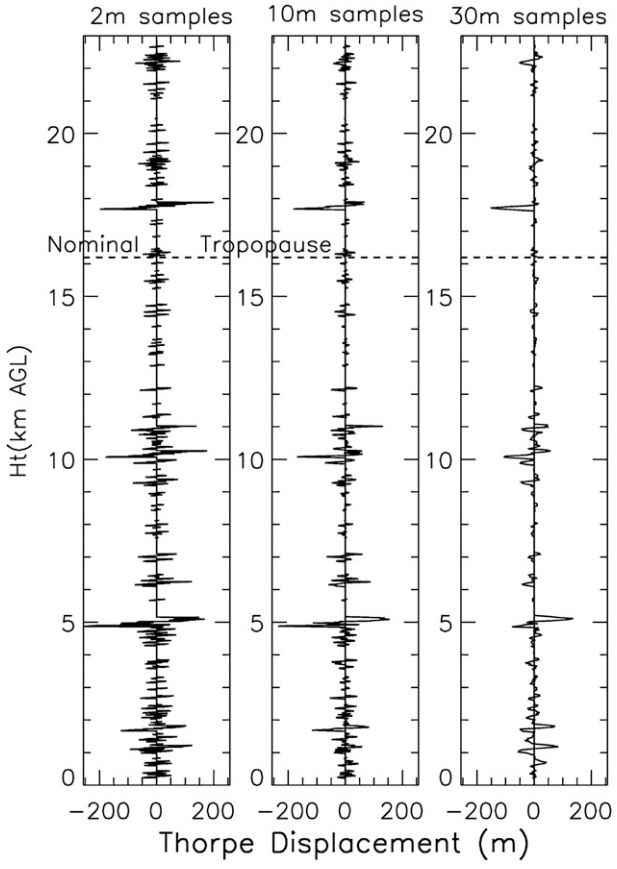

FIG. 5. (left) Example of three-point smoothed Thorpe displacements (overturning scales) covering the entire height range of a SAMS ascent. The mean ascent rate in this example is 2.1 m s^{-1}. (middle) As in (left), but sampled every 5 s (~10-m resolution) and (right) every 15 s (~30-m resolution).

nominal tropopause height around 16 km, as indicated by the horizontal dashed line).

The importance of the improved height resolution is illustrated in the three panels of Fig. 5. These panels show the results of sampling the same profile at 1 s (2.1-m resolution), 5 s (10.5-m resolution), and 15 s (31.5-m resolution). Note that these lower sampling rates correspond roughly to the vertical resolutions available from T-REX and FASTEX.

Examination of Fig. 5 clearly shows that the improved vertical resolution provided by the SAMS technique yields a significantly larger number of overturning events. Moreover, the magnitude of the Thorpe displacements is also a function of the vertical resolution.

5. Discussion

Based on the above results, it is possible to make a number of pertinent points relative to the feasibility of and need for employing SAMS radiosonde systems for high-resolution measurements of the troposphere and lower stratosphere. For convenience, these points have been separated into advantages and disadvantages.

a. Advantages

The results presented above suggest a number of potentially promising advantages in using SAMS. It appears feasible to obtain profile measurements with meter-scale vertical resolutions. Fundamentally, this capability enables studies of the small-scale dynamics throughout the atmosphere, a critical need evidenced by emerging atmospheric dynamic studies. These small-scale details include atmospheric overturnings, atmospheric gravity waves, scale-dependent gradient Richardson numbers, and the associated turbulence generation.

Because the SAMS technique employs standard radiosondes and conventional balloons, the primary difference is that the SAMS balloons require much less helium per launch. It is worth repeating here that the fundamental control for accurate rise rate lies not with the amount of helium but rather with a careful determination of net lift, as described in section 3.

It is also important to point out that the use of SAMS systems and the associated reduced balloon sizes result in reduced self-induced balloon motions and thereby provide a more accurate measurement of wind speeds (MacCready 1965; Wang et al. 2009). Smaller self-induced motions should also improve the accuracy of high-resolution velocity measurements, insofar as these motions produce incorrect readings.

Finally, a potentially important advantage to the SAMS technique is that both the measurable number of overturnings and the magnitude of the Thorpe displacements of overturnings are significantly enhanced by using higher-resolution data.

b. Disadvantages

One obvious result contained in the above discussions lies with the number of limitations arising from weather conditions, yet-to-be-determined sampling accuracies, and potential problems associated with sensor responses to slow-rise-rate conditions. Some of these limitations are easily overcome, whereas some significantly limit the application of SAMS radiosondes and others remain to be fully documented (and hopefully minimized).

The first clear limitation lies with the atmospheric conditions under which the SAMS technique can operate. Basically, because the ascent rates are in the range ~1 m s^{-1}, data acquisition during daytime convective conditions will be severely compromised. Benign nighttime conditions appear to be optimum for SAMS operations.

Second, as demonstrated herein, problems associated with the greatly increased ranges (weaker signals) and

extended operating times (battery limitations) associated with the slower ascent rates need to be improved. Potential solutions for these limitations could involve more sensitive telemetry systems and enhanced battery lifetimes.

Third, for optimal operations, it will be necessary to assess the potentially deleterious effects of the reduced ascent rates on the sensors resulting from decreased ventilation. These effects have yet to be fully investigated and will clearly be a function of the sensor design and of the type of sensor employed. The most obvious problem associated with decreased ventilation lies with the lack of humidity data.

Fourth, the capability of conventional radiosonde sensors to respond to rapid, small-scale wind fluctuations is, at best, poorly established. This capability may be even further compromised by using the reduced lifts and smaller balloon volumes associated with the SAMS technique.

Finally, the difficulty of preparing a SAMS system for launch is somewhat more onerous than that required for more conventional radiosonde launches. An accurate determination of the net lift of the entire SAMS package (± 5 g) is essential for a successful flight. In addition, because of the slower ascent rates, care must be taken to ensure that the launch site is clear of nearby obstructions (buildings, trees, power lines, etc.).

6. Conclusions

The SAMS technique, which incorporates conventional radiosonde capabilities with slower-rise-rate balloons, is capable of providing meter-scale vertical sampling throughout the troposphere and lower stratosphere. However, SAMS operation has a major limitation in that operations are problematic during periods of convective activity where local atmospheric motions typically exceed a fraction of the nominal 1 m s^{-1} mean radiosonde ascent rate. This restriction limits SAMS measurements primarily to nighttime operations. A series of unresolved potential problems remain that primarily pertain to the accuracy of the radiosonde sensors under slow-rise-rate conditions and to potential problems arising from the response of the total balloon–radiosonde package to small-scale wind fluctuations. These problems involve the effects of the reduced airflow past the package and the short-term dynamic response of the complete package.

It is important to stress that the results shown herein are based on a series of only 19 balloon launches made during relatively similar conditions. The intent of this campaign was to document the concept of using slow-rise-rate balloons to achieve improved vertical resolution under somewhat limited conditions. To quantify the accuracy of pressure, temperature, humidity, and wind determinations using SAMS launches will require a much larger series of SAMS launches made under a wide variety of conditions. Such an effort, although of considerable importance, is beyond the scope of the present effort.

Nevertheless, the growing need for meter-scale measurements throughout the lower atmosphere justifies our claim that there is an obvious niche in current atmospheric sampling technology for the SAMS technique. Indeed, given the availability of inexpensive digital storage capacity, even archiving all possible data from conventional radiosonde launches with ascent rates of 5 m s^{-1} would provide a wealth of useful data not currently available.

Although the potential problem of an evolving air mass during a balloon ascent is exacerbated by the use of slow-rise-rate balloons, SAMS launches provide a first look at overturning details that are not too different from those observed using more conventional systems. For example, although not presented here, similar overturns have been observed using very rapid descent (17 m s^{-1}) dropsonde data (F. Bocquet 2009, personal communication). In addition, overturns have been observed using essentially fixed-position tethered lifting system (TLS) balloons in the boundary layer (Sorbjan and Balsley 2009). Based on these results using relatively disparate techniques, it is reasonable to conclude that the overturns observed during SAMS flights are real and are indicative of small-scale, locally generated atmospheric processes.

Finally, the idea of a horizontal grid of simultaneous SAMS launches, where the data are archived aboard the individual sensors, would be instrumental in determining the three-dimensional structure of atmospheric overturns and their relationship to atmospheric gravity waves and local turbulence enhancements, as well as to other larger-scale phenomena.

Acknowledgments. We are pleased to acknowledge that this effort was supported by a small innovative research grant from CIRES (University of Colorado). We acknowledge with thanks the useful conversations with R. M. Jones, F. Bocquet, R. Frehlich, and D. David of CU-CIRES and Hal Cole of NCAR. Appreciation is extended to NOAA for the cooperation and the use of their ERIE field site, as well as to Dan Wolfe and Ludovic Bariteau of NOAA who provided valuable and whole-hearted help during the field campaign.

REFERENCES

Alford, M., and R. Pinkel, 2000: Observations of overturning in the thermocline: The context of ocean mixing. *J. Phys. Oceanogr.,* **30,** 805–832.

Balsley, B., M. Tjernström, and G. Svensson, 2008: On the scale dependence of the gradient Richardson number in the residual layer. *Bound.-Layer Meteor.,* **127,** 57–72.

Cho, J. Y. N., R. E. Newell, B. E. Anderson, J. D. W. Barrick, and K. L. Thornhill, 2003: Characterizations of tropospheric turbulence and stability layers from aircraft observations. *J. Geophys. Res.,* **108,** 8784, doi:10.1029/2002JD002820.

Clayson, C. A., and L. Kantha, 2008: On turbulence and mixing in the free atmosphere inferred from high-resolution soundings. *J. Atmos. Oceanic Technol.,* **25,** 833–852.

Fedorovich, E., R. Rotunno, and B. Stevens, Eds., 2004: *Atmospheric Turbulence and Mesoscale Meteorology*. Cambridge University Press, 280 pp.

Fritts, D., L. Wang, J. Werne, T. Lund, and K. Wan, 2009a: Gravity wave instability dynamics at high Reynolds numbers. Part I: Wave field evolution at large amplitudes and high frequencies. *J. Atmos. Sci.,* **66,** 1126–1148.

——, ——, ——, ——, and ——, 2009b: Gravity wave instability dynamics at high Reynolds numbers. Part II: Turbulence evolution, structure, and isotropy. *J. Atmos. Sci.,* **66,** 1149–1171.

Hock, T. F., and J. L. Franklin, 1999: The NCAR GPS dropwindsonde. *Bull. Amer. Meteor. Soc.,* **80,** 407–420.

MacCready, P. B., Jr., 1965: Comparison of some balloon techniques. *J. Appl. Meteor.,* **4,** 504–508.

Sorbjan, Z., and B. B. Balsley, 2009: Microstructure of turbulence in the stably stratified boundary layer. *Bound.-Layer Meteor.,* **129,** 191–210.

Thorpe, S., 1977: Turbulence and mixing in a Scottish loch. *Philos. Trans. Roy. Soc. London,* **286A,** 155–181.

Tjernström, M., B. B. Balsley, G. Svensson, and C. J. Nappo, 2009: The effect of critical layers on residual layer turbulence. *J. Atmos. Sci.,* **66,** 468–480.

Väisälä Corporation, 2006: Väisälä Radiosonde RS92-SGP brochure: Technical data. Väisälä Tech. Document B210358EN-C, 2 pp.

Wang, J., J. Bian, W. O. Brown, H. Cole, V. Grubišić, and K. Young, 2009: Vertical air motion from T-REX radiosondes and dropsonde data. *J. Atmos. Oceanic Technol.,* **26,** 928–942.

Werne, J., and D. Fritts, 1999: Stratified shear flow: Evolution and statistics. *Geophys. Res. Lett.,* **26,** 439–442.